

Pressure and Viscosity Effects on Thermal Geometrical Isomerization of Oxocarbocyanine Cations¹

Jong Chul Kim, Yasushi Ohga, Tsutomu Asano,* Noham N. Weinberg,*[†] and Adrian V. George^{††,2}

Department of Applied Chemistry, Faculty of Engineering, Oita University, 700 Dannoharu Oita 870-1192

[†]Department of Chemistry, University College of the Fraser Valley, 33844 King Road, Abbotsford, B.C. V2S 7M9, Canada

^{††}Department of Organic Chemistry, School of Chemistry, The University of Sydney, Sydney, NSW 2006, Australia

(Received May 22, 2000)

Pressure and viscosity effects on the rate of thermal *Z/E* isomerization of two carbocyanine dyes, 3,3'-diethyloxocarbocyanine iodide (DOCI) and 3,3'-diethyloxadiazocarbocyanine iodide (DODCI) were measured in 2-methylpentane-2,4-diol. From the results, the following conclusions are obtained. 1. The medium and the chemical coordinates have to be treated separately, as in the reactions of uncharged species. 2. A positive charge on the reactant seems to induce an earlier deviation from the transition state theory. 3. The most important factors controlling a deviation from the transition state theory are the anisotropy of the characteristic times of reaction and solvent fluctuations, and the strength of the solute-solvent interactions.

Dependence of reaction rates on the solvent has been one of the main subjects of research in organic chemistry. Such dependence comes from two sources, static and dynamic. The static effects represent the equilibrium effects of medium on the shape of the potential energy surface, whereas the dynamic effects reflect the difference in the relative time scales of the chemical conversion of the reaction system and the thermal fluctuations of the solvent. If the solvent thermal fluctuations are fast enough, the solvent can instantly adjust to the evolution of the reaction system. As a result, no strains and misfits develop between reactant and solvent in the course of the reaction, and most molecules overcome the reaction barrier near the lowest point of the ridge separating the reactant and the product valley, the transition state. In this case, the transition state theory (TST) is valid and the observed rate constant, k_{obs} , is well-represented by the TST rate constant, k_{TST} :

$$k_{\text{obs}} = k_{\text{TST}} \quad (1)$$

If solvent thermal motion is not sufficiently fast, the supply of the reactant molecule to the saddle point can become too slow to maintain the equilibrium distribution of the reactant and we start observing dynamic effects of the rate of the solvent thermal fluctuations on the reaction rate. The thermal fluctuation rate is inversely proportional to the friction between the solvent molecules which, in turn, may be considered to be proportional to the solvent viscosity η .³ Therefore, the TST is anticipated to fail at relatively high viscosities. Under such conditions, the rate constant is expected to decrease with increasing η .

Although it has been known for many years that the viscosity of organic liquids rapidly increases with increasing pres-

sure,⁴ the viscosity effects were invoked only in limited cases such as reactions involving reactive free radicals.⁵ For most thermal reactions in common solvents, the solvent thermal motions are fast enough to maintain Boltzmann distribution, and thus in most cases the solvent effects can be discussed in terms of the TST as the difference in solvation of the initial and the transition state.⁶ Correspondingly, the kinetic effects of pressure can also be discussed in terms of the activation volume ΔV^\ddagger , a partial molar volume difference between the reactant and the activated complex:

$$\left(\frac{\partial \ln k}{\partial P} \right)_T = - \frac{\Delta V^\ddagger}{RT} \quad (2)$$

The TST interpretation of high-pressure kinetic effects was firmly established at a relatively early stage of the high-pressure studies,⁷⁻⁹ and thousands of cases were rationalized on the basis of the structure and the solvation changes of the reactant(s) during the activation step.⁹⁻¹²

In the study of pressure effects, it is important to separate the dynamic effects from the static ones. The following procedure may be used for isolating the dynamic solvent effects from the overall kinetic effects of pressure. Suppose that for a particular reaction the TST is valid at low pressures. Thus, at the beginning of pressurization, an increase in pressure will result in a change in the rate constant according to Eq. 2. That is, a reaction will be accelerated or decelerated depending on whether the activation volume is negative or positive. At sufficiently higher pressures, however, the solvent becomes so viscous that it causes all reactions, independently of the sign of the activation volume, to slow down. The TST-based pressure effect may

be extrapolated to these TST-invalid viscosities if the same reaction mechanism holds at all pressures. This extrapolation provides an estimate for the TST-expected rate constant k_{TST} , and the magnitude of dynamic solvent effects can be estimated by the ratio $k_{\text{obs}}/k_{\text{TST}}$. This approach has been employed in our earlier studies of high-pressure effects on the thermal *Z/E* isomerization of substituted benzaldehyde anils (**1–3**) and azobenzenes (**4, 5**).^{13–15} A similar study has also been performed for the degenerate isomerization of a hexafluoroacetone anil **6** (Chart 1).¹⁶ The half-lives of these reactions ranged

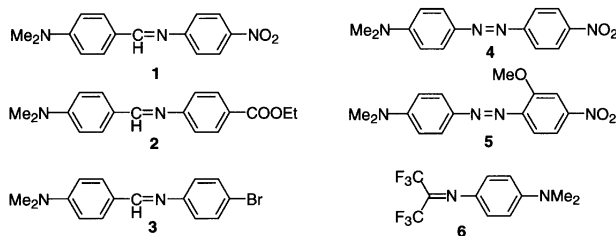


Chart 1.

from milliseconds to seconds and the pressure effects in common solvents reflected the reaction mechanisms.^{17–19} In all of these studies, viscous liquids with branched molecular structures, such as 2-methylpentane-2,4-diol (MPD),¹⁴ glycerol triacetate (GTA),¹³ and 2,4-dicyclohexyl-2-methylpentane (DCMP),¹⁵ were used as solvents. The pressure dependencies of the viscosity η of these liquids were approximately given by Eq. 3 where η_P and $\eta_{0.1}$ are the viscosities at pressures P and 0.1 MPa, respectively. The pressure coefficient α was greater in these viscous solvents than in common ones.^{4,14,15,20}

$$\eta_P = \eta_{0.1} e^{\alpha P} \quad (3)$$

As expected, although the TST proved to be valid for these slow thermal reactions at low pressure conditions, the dynamic solvent effects were observed at higher pressures in the form of a pressure-induced retardation that could not be rationalized within the framework of the TST.

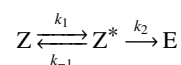
Theoretical models that describe the dynamic effects of solvents may be divided into two groups — one- and two-dimensional — depending on the number of coordinates explicitly used to describe the reaction. In the former, originally proposed by Kramers and later modified by Grote and Hynes (the KGH model),^{21–23} the progress of reaction is described by a single coordinate representing a concerted motion of both the reaction system and the solvent. In the framework of this model,

$$k_{\text{obs}} = k_{\text{TST}} f(\eta) \quad (4)$$

and thus the isoviscous temperature dependence of the KGH k_{obs} is expected to be characterized by the same activation energy as that of k_{TST} . It has been shown, however, that in the reactions studied so far^{13–15} the isoviscous temperature dependence of k_{obs} decreases with increasing viscosity in the TST-invalid viscosity region, contrary to what is expected in the KGH model.

In a two-dimensional model, proposed by Agmon and Hopfield (the AH model)^{24,25} and further developed by Sumi and Marcus,²⁶ the reaction system and the solvent are described by two independent coordinates, and, if the solvent thermal

fluctuations are not fast enough, solvent rearrangement around the reactant system may become rate-determining. The overall reaction in the AH model is represented by an ensemble of simultaneous reactions taking place at various configurations of solvent. The fastest of these is the process at the solvent configuration favoring the transition state. As a result, the relative population of such solvent configurations gets depleted faster than other ones and needs to be recovered through a diffusion-like solvent rearrangement. As long as the latter is sufficiently fast, the predominant contribution to the overall process comes from the barrier crossing near the transition state and thus the reaction is described by the TST. If, however, the solvent thermal fluctuations are not fast enough, they cannot fully recover the equilibrium distribution of the solvent configurations and the major contribution to the overall process shifts away from the transition state region. The overall process can be represented in an approximate form, as shown in Scheme 1.¹³



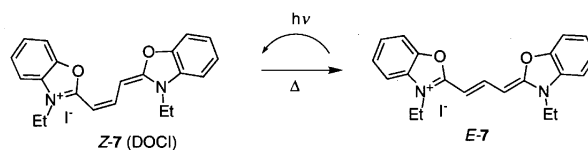
Scheme 1.

The first step in Scheme 1 describes a diffusion along the medium coordinate (a solvent rearrangement) uphill from the reactant minimum Z to the intermediate Z^* which represents the configuration of the solvated reactant with the highest contribution to the energy barrier crossing; the second step describes the chemical conversion into the product E that takes place at a fixed configuration of solvent. At a given temperature and a viscosity, the position of Z^* is fixed on the medium coordinate, but it is expected to change if the parameters are changed. It has been demonstrated by Sumi²⁷ that in the steady state approximation

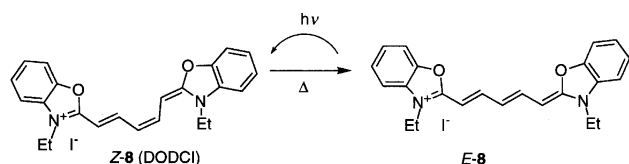
$$\frac{1}{k_{\text{obs}}} = \frac{1}{k_f} + \frac{1}{k_{\text{TST}}} \quad (5)$$

where k_f is a high-viscosity limit of k_{obs} in the TST-invalid region.²⁸ The validity of Eq. 5 is supported by the exact numerical solutions^{29,30} obtained for the AH model in a wide range of characteristic parameters. Equation 5 allows one to estimate the fluctuation-limited rate constant k_f from k_{obs} and k_{TST} . As expected for a fluctuation-limited rate process, linear Arrhenius plots and inverse fractional power viscosity dependence were observed for k_f .^{13–15}

Solvent thermal fluctuations are expected to be influenced by the existence of an electrical charge on the reactant. A stronger solute-solvent interaction in an ionic solute will result in a failure of the TST at lower viscosities. If this expectation is met, the results will give us further insight into the dynamic course of solution reactions. This paper reports the pressure and the viscosity effects on the *Z/E* isomerization of two carbocyanine cations **7** and **8**, shown in Schemes 2 and 3, respectively.^{1,31}



Scheme 2.



Scheme 3.

Experimental

Materials. 3,3'-Diethyloxacarbocyanine iodide **7** (DOCI) and 3,3'-diethyloxadicarbocyanine iodide **8** (DODCI) were commercial products (Aldrich) and were used as received. 2-Methylpentane-2,4-diol was a product of Wako Pure Chemical and was used after distillation (105.5–106 °C/21 mmHg).

High-Pressure Kinetics. Thermally unstable Z-isomer was formed photochemically and its decay was followed by monitoring the absorbance at λ_{\max} of the E-isomer. The details of the high-pressure vessel were described previously.³⁴ The reactions followed the first-order kinetics at all of the conditions studied. The standard deviation of the observed rate constant k_{obs} was usually less than 1% of the value at 0.1 MPa and it increased gradually with increasing pressure because of a decrease in the quantum yield of the photoconversion and it finally reached around 10% at the highest viscosity. The standard deviations in the calculated values of activation volumes were $\pm 0.2 \text{ cm}^3 \text{ mol}^{-1}$ or smaller and those in the activation energies were as given in the tables.

Results and Discussion

Kinetic Effects of Pressure. The k_{obs} values for the isomerization of DOCI in MPD are listed in Table 1 and are plotted in Fig. 1 against the pressure. The data include the results obtained in ethanol at 25 °C. Ethanol, a solvent with a polarity similar to that of MPD and yet of a much lower viscosity,^{14,20} was used to estimate the TST-expected pressure effects.

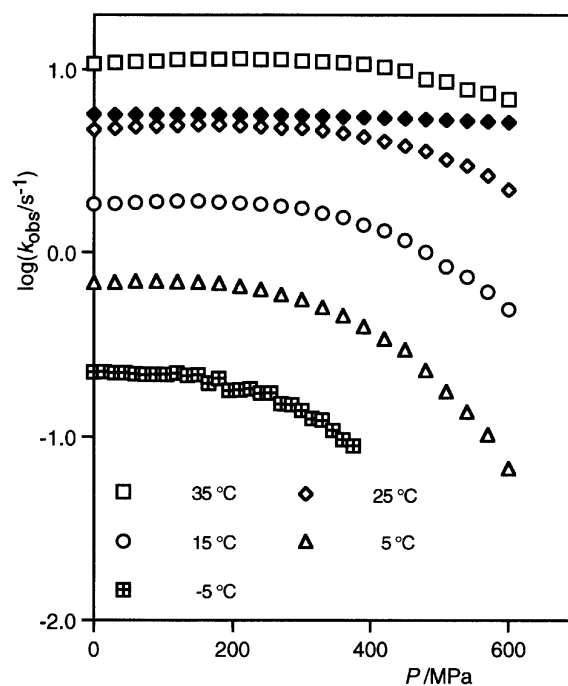


Fig. 1. Pressure effects on the isomerization rate of DOCI in MPD (open symbols) and ethanol (closed symbol) at various temperatures.

The dielectric constants are 25.86 for MPD (20 °C) and 24.55 for ethanol (25 °C).³⁵ As it can be clearly seen from Fig. 1, the rate constants and their pressure dependencies are similar in the two solvents at pressures lower than 200 MPa, a strong indication of the absence of the viscosity-induced retardations in MPD. The activation volumes calculated by assuming a linear

Table 1. The First-Order Rate Constants ($k_{\text{obs}}/\text{s}^{-1}$) for the Isomerization of DOCI in MPD and Ethanol at Various Temperatures and Pressures

P/MPa	MPD					EtOH
	-5 °C	5 °C	15 °C	25 °C	35 °C	25 °C
0.1	0.225	0.687	1.84	4.72	10.8	5.71
30	0.223	0.693	1.85	4.79	10.9	5.68
60	0.221	0.699	1.88	4.88	11.1	5.70
90	0.219	0.700	1.89	4.94	11.1	5.70
120	0.223	0.697	1.91	4.96	11.3	5.69
150	0.218	0.692	1.91	5.00	11.4	5.69
180	0.208	0.684	1.89	5.00	11.5	5.68
210	0.181	0.656	1.87	4.95	11.5	5.67
240	0.173	0.631	1.84	4.88	11.4	5.65
270	0.151	0.595	1.79	4.80	11.4	5.64
300	0.139	0.556	1.75	4.78	11.1	5.60
330	0.123	0.505	1.63	4.65	11.1	5.57
360	0.0967	0.456	1.55	4.49	10.9	5.53
390		0.399	1.42	4.29	10.7	5.50
420		0.340	1.32	4.06	10.3	5.45
450		0.298	1.16	3.82	9.87	5.41
480		0.230	1.00	3.58	8.83	5.36
510		0.176	0.841	3.23	8.61	5.31
540		0.137	0.737	2.97	7.77	5.26
570		0.103	0.613	2.64	7.40	5.21
600		0.0673	0.491	2.20	6.89	5.15

dependence of $\ln k_{\text{obs}}$ on the pressure are listed in Table 2. All activation volumes are close to zero, in agreement with the results of Laser-Induced Opto-Acoustic Spectroscopy (LIOAS) by Braslavsky and co-workers,³⁶ who observed little volume difference between the *E*- and the *Z*-isomer. This allows us to conclude that the partial molar volume of the reactant stays almost unchanged during the whole process of the thermal isomerization.

The results for DODCI shown in Table 3 and Fig. 2 were qualitatively different from those for DOCI in two aspects: the activation volume was positive and the downward deviations of the rates in MPD from those in ethanol appeared at much lower pressures. In this case again, the atmospheric rate constants and the initial pressure effects in MPD were very close to the ones in ethanol, suggesting the validity of the TST in MPD at 0.1 MPa. However, whereas the $\log k_{\text{obs}}-P$ plots for ethanol were concave-up, as expected for a reaction with a positive activation volume,³⁷ in the case of MPD, these plots were concave-down, i.e. the absolute magnitude of the pressure effect kept increasing in the whole pressure range. The MPD plots deviate from the ethanol curves earlier, i.e. at lower pressures in DODCI than in DOCI. The most reasonable explanation of this difference is that viscosity-induced retardations appear at lower

pressures in DODCI than in DOCI. The activation volumes at 0.1 MPa, ΔV_0^\ddagger , in ethanol were obtained by fitting the results into Eq. 6^{34,38} with adjustable parameters *a*, *b*, and *c*. These values are listed in Table 4 along with the average activation volume $\Delta \bar{V}^\ddagger$ between 0.1 and 30 MPa (Eq. 7) in MPD.

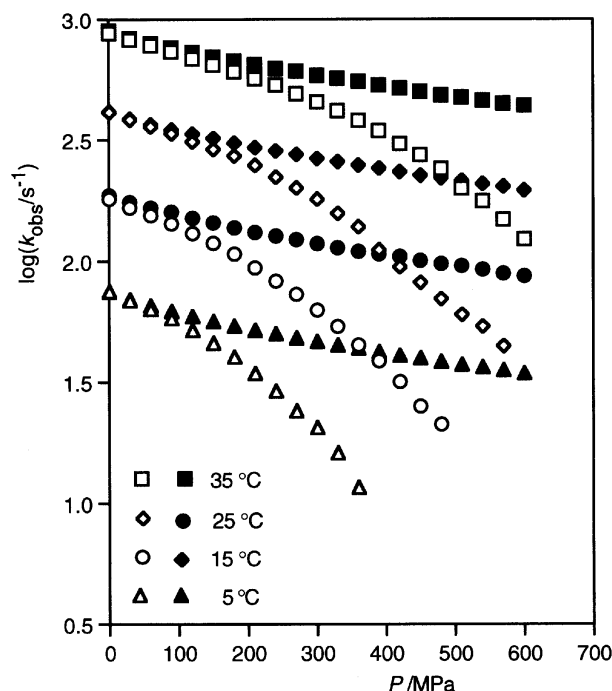


Fig. 2. Pressure effects on the isomerization rate of DODCI in MPD (open symbols) and ethanol (closed symbols) at various temperatures.

Table 2. Activation Volumes ($\Delta V^\ddagger/\text{cm}^3 \text{ mol}^{-1}$) for the *Z/E* Isomerization of DOCI in MPD and Ethanol at Various Temperatures

$T/^\circ\text{C}$	MPD					EtOH
	-5	5	15	25	35	25
ΔV^\ddagger	0.4	0.0	-0.5	-0.8	-0.6	0.4

Table 3. The First-Order Rate Constants ($k_{\text{obs}}/\text{s}^{-1}$) for the Isomerization of DODCI in MPD and Ethanol at Various Temperatures and Pressures

P/MPa	MPD				EtOH			
	5 °C	15 °C	25 °C	35 °C	5 °C	15 °C	25 °C	35 °C
0.1	75.0	180	412	875	74.7	186	414	897
30	68.7	166	384	820	69.5	175	387	833
60	63.2	155	360	779	65.5	166	367	794
90	57.9	143	337	736	62.2	160	350	761
120	51.8	130	312	686	59.2	151	336	731
150	45.9	118	290	647	56.3	144	322	698
180	40.3	107	272	608	53.9	137	308	672
210	34.4	94.0	249	567	51.8	132	295	650
240	29.0	82.8	222	534	50.0	127	285	624
270	23.9	72.9	200	493	48.1	123	276	609
300	20.5	62.6	180	456	46.6	118	266	587
330	16.1	53.6	158	418	44.9	114	258	569
360	11.7	44.9	138	382	43.6	110	249	552
390		38.6	111	347	42.2	107	242	536
420		31.6	94.6	305	40.8	104	234	520
450		25.1	81.6	274	39.7	101	226	501
480		21.1	69.9	241	38.5	97.5	221	485
510			60.1	200	37.3	95.7	215	476
540			53.7	177	36.4	92.5	208	461
570			44.5	149	35.4	88.9	203	449
600				123	34.4	86.9	196	440

Table 4. Activation Volumes ($\Delta V^\ddagger/\text{cm}^3 \text{ mol}^{-1}$) for the Z/E Isomerization of DODCI in MPD and Ethanol at Various Temperatures

T/°C	$\Delta \bar{V}^\ddagger$ in MPD				ΔV_0^\ddagger in EtOH ^{a)}			
	5	15	25	35	5	15	25	35
ΔV^\ddagger	5.5	4.8	5.2	5.6	5.9	5.0	5.6	6.5

a) $\Delta V_0^\ddagger = -(a + bc)RT$.

$$\ln \frac{k_p}{k_{0.1}} = aP + b \ln(1 + cP) \quad (6)$$

$$\Delta \bar{V}^\ddagger = -\frac{RT}{30} \ln \frac{k_{30}}{k_{0.1}} \quad (7)$$

The positive values are again compatible with the results of LIOAS measurements. According to Braslavsky,³⁶ the partial molar volume of the cation decreases in the E to Z isomerization by 30–50 $\text{cm}^3 \text{ mol}^{-1}$. This surprisingly large volume difference between the two geometrical isomers was attributed to the solvation difference caused by different “polarities” in the two isomers.

Dynamic Solvent Effects. Figures 3 and 4 show plots of the k_{obs} values against η . As observed in the systems studied previously, the isoviscous temperature dependence shows a small but clear tendency to decrease with increasing η . The isoviscous activation energies are listed in Table 5 and the isobaric values are given in Table 6 for comparison. Since the activation volume for DOCI is close to zero, the isoviscous and isobaric activation energies are similar at the TST-valid conditions. In DODCI, on the other hand, the former are somewhat

smaller because of a positive activation volume (Compare Figs. 2 and 4.). In both cyanine cations the isoviscous activation energy decreases with increasing η , while the isobaric activation energy shows only a minor dependence on the pressure.³⁹ These results cannot be rationalized on the basis of the KGH model and strongly suggest a necessity to treat the medium and the chemical coordinates separately.

Analysis Based on the AH Model. In order to examine the validity of Scheme 1 in the present reactions, the fluctuation-limited rate constant k_f were calculated on the basis of Eq. 5. In DOCI, the k_{TST} values at high viscosities were estimated by linear extrapolations of the lower-pressure data. In DODCI, the dynamic solvent effects were observed at relatively low pressures and the k_{TST} values could not be estimated by such an extrapolation. The results in ethanol were used instead. Namely, the rate constants in ethanol were fitted to Eq. 6 and the same function was assumed to describe the TST-based pressure effects in MPD. The k_f values thus obtained are plotted against the viscosity in Figs. 5 and 6. As observed in the previous cases,^{13–15} the plots were satisfactorily linear and the rate constant was inversely proportional to a fractional power of η :

$$k_f \propto \eta^{-\beta} \quad \beta < 1. \quad (8)$$

Furthermore, the Arrhenius plots were again reasonably linear (*vide infra*), similar to what was observed in the previous studies. These results seem to confirm the validity of Scheme 1 as a model for the present reaction systems.

Figures 5 and 6 clearly indicate that k_f demonstrates a temperature dependence at isoviscous conditions. The respective isoviscous Arrhenius plots are shown in Figs. 7 and 8 along

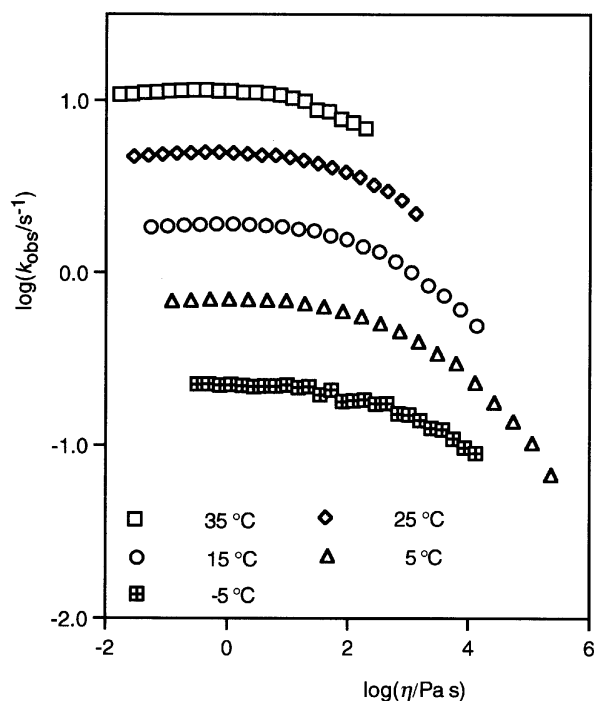


Fig. 3. Viscosity dependence of the isomerization rate of DOCI in MPD at various temperatures.

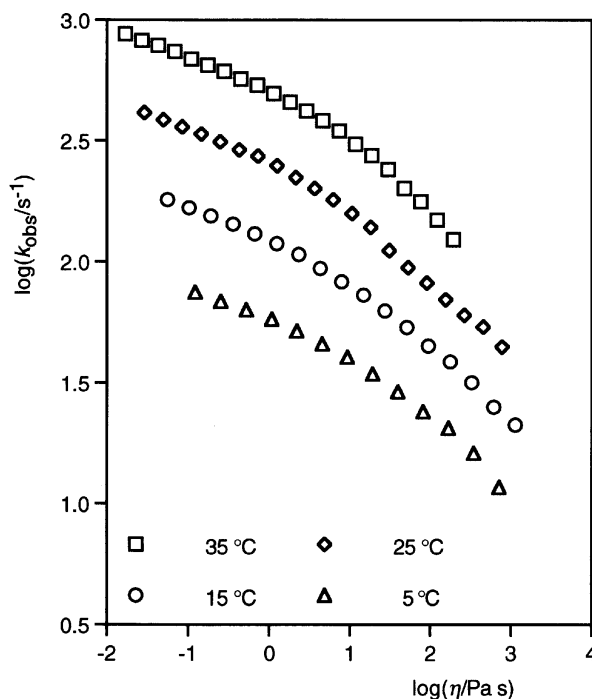


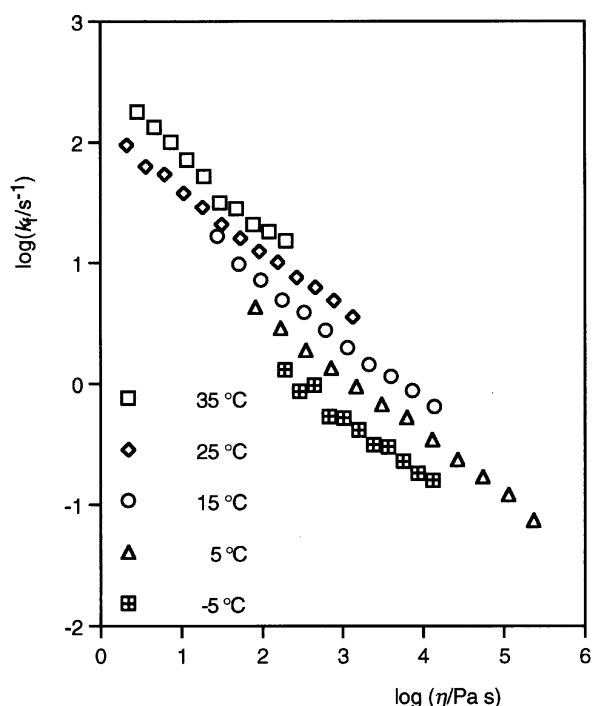
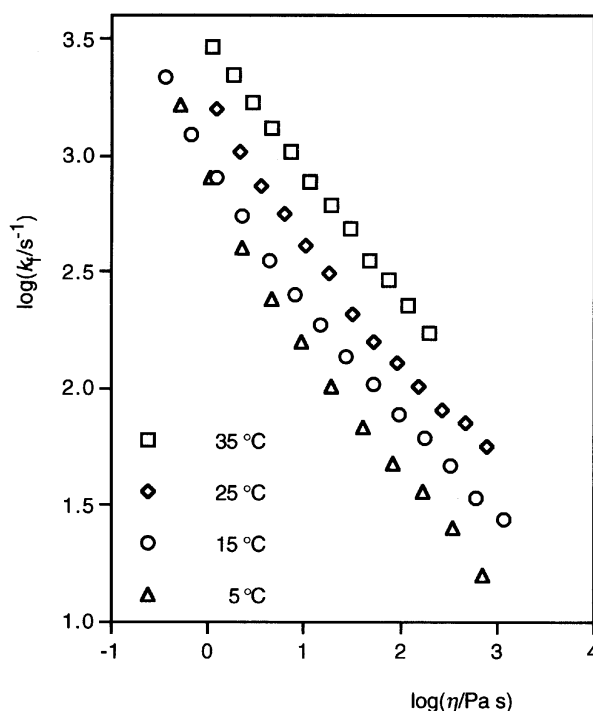
Fig. 4. Viscosity dependence of the isomerization rate of DODCI in MPD at various temperatures.

Table 5. Isoviscous Activation Energies ($E_a/kJ\ mol^{-1}$) from k_{obs} for the Isomerization of DOCI and DODCI in MPD

$\eta/Pa\ s$	0.1	1	10	10^2	10^3	10^4
DOCI	67.2 ± 0.5	67.6 ± 0.6	66.5 ± 1.0	63.7 ± 1.4	58.8 ± 2.1	51.6 ± 2.1
DODCI	52.7 ± 0.1	49.3 ± 0.8	45.8 ± 1.3	42.2 ± 1.0		

Table 6. Isobaric Activation Energies ($E_a/kJ\ mol^{-1}$) from k_{obs} for the Isomerization of DOCI and DODCI in MPD

P/MPa	0.1	30	60	90	120	150
DOCI	66.5 ± 0.5	66.8 ± 0.7	67.3 ± 0.8	67.4 ± 1.0	67.6 ± 0.7	68.1 ± 0.8
DODCI	58.5 ± 0.2	59.1 ± 0.5	59.9 ± 0.5	60.8 ± 1.3		

Fig. 5. Viscosity dependence of the fluctuation-limited rate constant k_f in the isomerization of DOCI in MPD.Fig. 6. Viscosity dependence of the fluctuation-limited rate constant k_f in the isomerization of DODCI in MPD.

with a few isobaric plots. Table 7 lists the isoviscous activation energies E_{a_f} together with the isoviscous $E_{a_{TST}}$. The corresponding data for the azobenzenes studied previously are listed in Table 8. Table 7 reveals that, both in DOCI and DODCI, the isoviscous activation energies E_{a_f} are smaller than the isoviscous $E_{a_{TST}}$. This does not mean, however, that the reaction barriers in the TST-invalid viscosity region are lower than the TST barriers, as this would be interpreted if the effect were static rather than dynamic. In fact, the situation is just the opposite, since any non-TST flux would have to cross the barrier at a point higher than the TST saddle point. This apparent contradiction stems from the fact that the isoviscous activation energies E_{a_f} do not measure the height of the reaction barrier: they merely reflect the overall effect of temperature on the complex process described by Scheme 1. Indeed, let Z_1^* be a location of configuration Z^* on solvent coordinate at a given viscosity η and a temperature T_1 . If at a constant viscosity the temperature is increased to its new value, T_2 , the reaction $Z_1^* \rightarrow E$ accelerates, and, since the rate of the solvent rearrangement remains

the same under isoviscous conditions, this leads to a depletion of the population of the Z_1^* configuration. As a result, an earlier configuration of the solvated reactant, Z_2^* , will contribute the most to the overall reaction flux, i.e. Z^* shifts from Z_1^* to Z_2^* further away from the TS region, thus further reducing the k_f/k_{TST} ratio. Thus,

$$\left(\frac{\partial}{\partial T} \frac{k_f}{k_{TST}}\right)_\eta < 0. \quad (9)$$

The isoviscous activation energies E_{a_f} and $E_{a_{TST}}$ can be expressed as temperature derivatives of the logarithms of the respective rate constants, k_f and k_{TST} :

$$E_{a_f} = RT^2 \left(\frac{\partial \ln k_f}{\partial T}\right)_\eta \quad (10)$$

$$E_{a_{TST}} = RT^2 \left(\frac{\partial \ln k_{TST}}{\partial T}\right)_\eta. \quad (11)$$

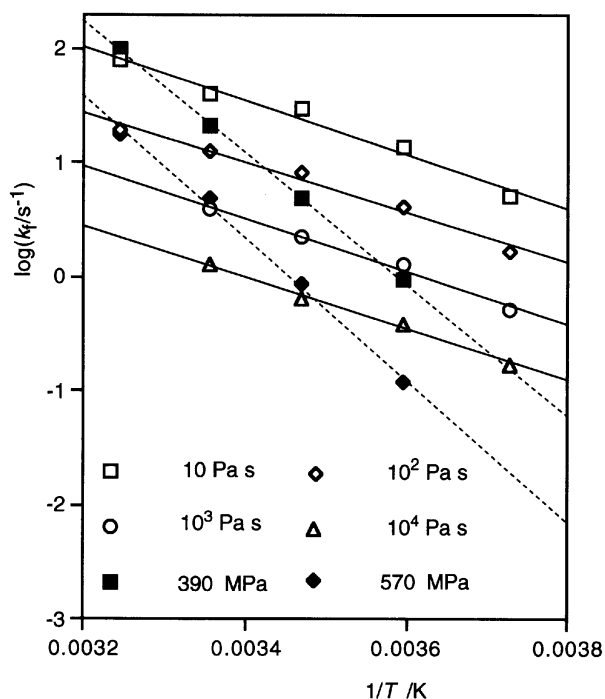


Fig. 7. Isoviscous (open symbols) and isobaric (closed symbols) Arrhenius plots for the fluctuation-limited rate constant k_f in the isomerization of DOCI in MPD.

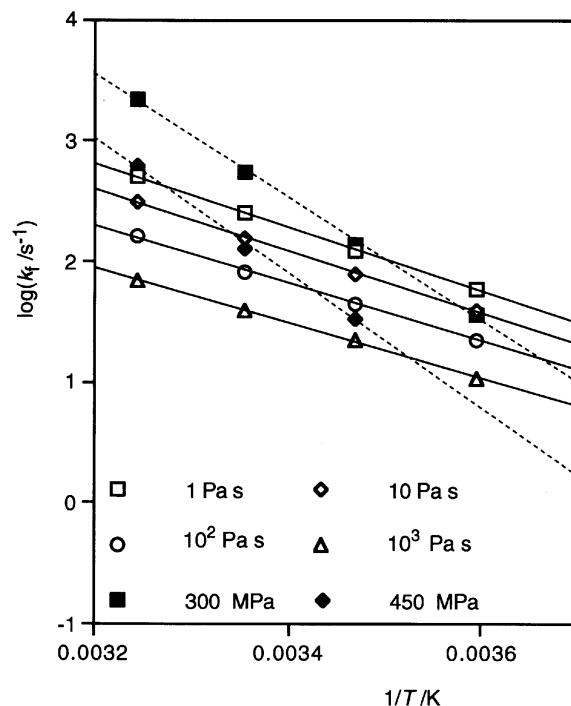


Fig. 8. Isoviscous (open symbols) and isobaric (closed symbols) Arrhenius plots for the fluctuation-limited rate constant k_f in the isomerization of DODCI in MPD.

Therefore,

$$Ea_f = Ea_{TST} + RT^2 \left(\frac{\partial}{\partial T} \ln \frac{k_f}{k_{TST}} \right)_\eta \quad (12)$$

By virtue of Eq. 9, the second term in the right-hand side of Eq. 12 is negative and thus $Ea_f < Ea_{TST}$. In other words, the isoviscous temperature dependence of k_f is expected to be weaker than that of k_{TST} , in agreement with the data presented in Tables 7 and 8. The ratio $r = Ea_f/Ea_{TST}$ describes the temperature dependence of the ratio k_f/k_{TST} : the stronger this dependence, the

further the r deviates from 1. The viscosity dependence of r seems to be different in the charged (Table 7) and the uncharged (Table 8) reactants.

The above results clearly indicate that both temperature and viscosity are important parameters determining when the dynamic effects of solvation become essential. The appearance of these effects depends on the relative time scale of the chemical conversion characterized by k_{TST} and the solvent thermal fluctuations determined by η . It has been shown earlier^{29,30} that the product $k_{TST}\eta$ can be used in the AH model to describe the bal-

Table 7. Isoviscous Activation Energies from k_f ($Ea_f/\text{kJ mol}^{-1}$) and k_{TST} ($Ea_{TST}/\text{kJ mol}^{-1}$) and Their Ratios in the Isomerization of DOCI and DODCI in MPD

$\eta/\text{Pa s}$	DOCI			DODCI		
	Ea_f	Ea_{TST}	$r (=Ea_f/Ea_{TST})$	Ea_f	Ea_{TST}	$r (=Ea_f/Ea_{TST})$
1				41±1.0	51±0.2	0.80
10	45±3.7	69±0.8	0.65	41±1.0	49±0.1	0.84
10 ²	42±3.2	70±1.0	0.60	40±0.9	46±0.1	0.87
10 ³	43±2.4	71±1.2	0.61	39±0.7	44±0.1	0.89
10 ⁴	44±2.1	72±1.4	0.61			

Table 8. Isoviscous Activation Energies from k_f ($Ea_f/\text{kJ mol}^{-1}$) and k_{TST} ($Ea_{TST}/\text{kJ mol}^{-1}$) and Their Ratios in the Isomerization of 4 and 5 in MPD

$\eta/\text{Pa s}$	4			5		
	Ea_f	Ea_{TST}	$r (=Ea_f/Ea_{TST})$	Ea_f	Ea_{TST}	$r (=Ea_f/Ea_{TST})$
10	56±6.2	69±0.8	0.81	58±3.7	70±0.2	0.83
10 ²	50±4.4	69±1.3	0.72	54±2.6	71±0.5	0.76
10 ³	45±3.1	69±3.1	0.65	50±1.9	72±0.6	0.69
10 ⁴	45±0.8	69±2.0	0.65	46±1.8	70±1.9	0.66

ance of the characteristic times of the reaction system and the solvent : the greater the product $k_{\text{TST}}\eta$, the higher the anisotropy of characteristic times of the reaction system and the solvent and thus the stronger the dynamic solvent effects. The plots of $\log(k_{\text{obs}}/k_{\text{TST}})$ vs. $\log(k_{\text{TST}}\eta)$ for DOCI and DODCI are presented in Fig. 9. As expected in the AH model, the results obtained at different temperatures fall on the same curve when plotted in these coordinates. The quality of the aggregation is higher for DOCI. The DODCI points are somewhat scattered, which can be attributed to the fact that the k_{TST} values, essential for the plot, were estimated from the ethanol data. Interestingly, the DOCI and DODCI points fall practically on the same curve when plotted in the $\log(k_{\text{obs}}/k_{\text{TST}}) - \log(k_{\text{TST}}\eta)$ coordinates, whereas they show a significant difference when plotted in $\log k_{\text{obs}} - \log \eta$ coordinates (Figs. 3 and 4). This could be anticipated, since a faster reaction of DODCI is expected to display a non-TST behavior at lower viscosities.

Figure 10 shows the plots for **2**, **4** and DOCI. It can be clearly seen that the deviations from the TST appear at lower $k_{\text{TST}}\eta$ values in the carbocyanine cation. Similar plots for DODCI and other neutral reactants also show the same tendency : deviations from TST appear at lower $k_{\text{TST}}\eta$ values in the carbocyanines than in the neutral reactants. The most probable source of this distinction is the difference in reorganization energy. The latter is another important parameter of the AH model and is defined as the energy difference between Z and Z*_{TST} configurations of solvated reactant (Scheme 1). The $k_{\text{obs}}/k_{\text{TST}}$ ratio has been shown²⁹ to depend exponentially on reorganization energy and to change by several orders of magnitude upon its variation. A positive charge on the reactant seems to induce an earlier

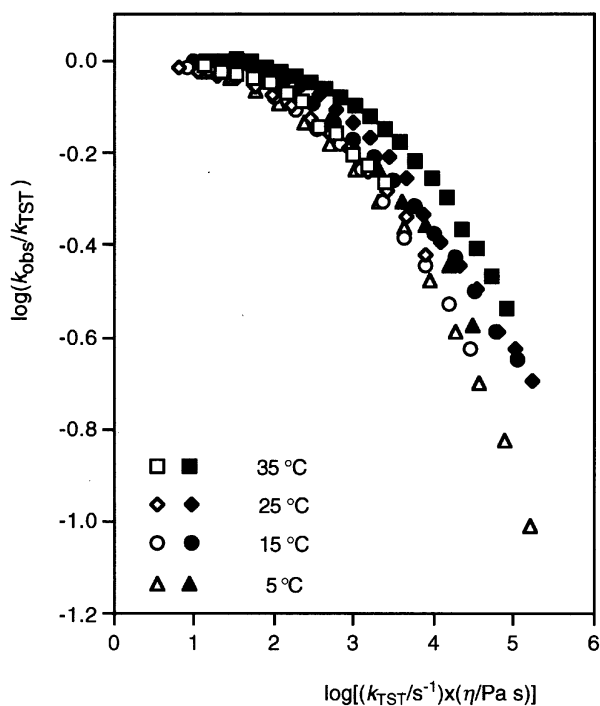


Fig. 9. Dependence of $\log(k_{\text{obs}}/k_{\text{TST}})$ on $\log(k_{\text{TST}} \times \eta)$ for the isomerization of DOCI (open symbols) and DODCI (closed symbols) at various temperatures.

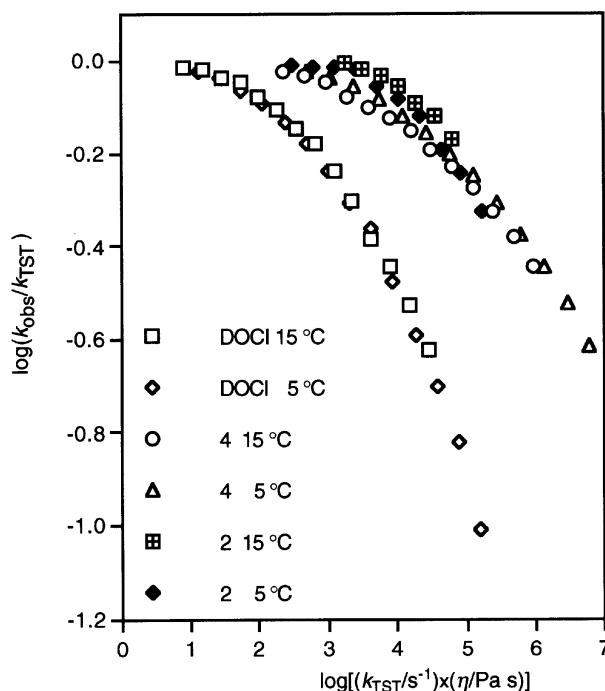


Fig. 10. A comparison of $\log(k_{\text{obs}}/k_{\text{TST}}) - \log(k_{\text{TST}} \times \eta)$ plots for DOCI and neutral reactants.

er deviation from the TST, in full agreement with the expectation that charged molecules interact stronger with a solvent and thus should be characterized by a greater reorganization energy.

Conclusions

The experimental results presented here again strongly suggest the general validity of the AH model for the description of the dynamic solvent effects. Two parameters of the model—the anisotropy of the characteristic times of the reaction system and solvent described by the product $k_{\text{TST}}\eta$ and the reorganization energy—control the strength of these effects, as measured by the ratio $k_{\text{obs}}/k_{\text{TST}}$. A positive charge on the reactant seems to induce an earlier deviation from the TST.

This work was partly supported by a Grant-in Aid for Scientific Research from the Ministry of Education, Science, Sports and Culture (No. 08454204). Financial support by JSPS to AVG is gratefully acknowledged.

References

- 1 A part of the experimental results in this paper was published in, J. C. Kim, Y. Ohga, and T. Asano, *Chem. Lett.*, **1999**, 301.
- 2 JSPS Fellow (1996).
- 3 This proportionality does not seem to hold in polymeric media. A. Shuto, T. Takahashi, Y. Ohga, T. Asano, H. Saito, K. Matsuo, and H.-D. Lüdemann. *Z. Naturforsch.*, **55a**, 616 (2000).
- 4 For examples, see Chapter XII in, P. W. Bridgman, "The Physics of High Pressure," Bell, London (1949).
- 5 For example, the termination process in neat polymeriza-

tion of ethylene was moderately retarded by pressure ($\Delta V^\ddagger = 7 \text{ cm}^3 \text{ mol}^{-1}$) and it was attributed to a retardation of translational diffusion by an increase in the viscosity. P.-C. Lim and G. Luft, *Makromol. Chem.*, **184**, 849 (1983).

6 C. Reichardt, "Solvents and Solvent Effects in Organic Chemistry," 2nd ed, VCH, New York (1988).

7 S. D. Hamann, "Physico-Chemical Effects of Pressure," Butterworths, London (1957).

8 E. Whalley, *Adv. Phys. Org. Chem.*, **2**, 93 (1964).

9 W. J. le Noble, *Prog. Phys. Org. Chem.*, **5**, 207 (1967).

10 T. Asano and W. J. le Noble, *Chem. Rev.*, **78**, 407 (1978).

11 R. van Eldik, T. Asano, and W. J. le Noble, *Chem. Rev.*, **89**, 549 (1989).

12 A. Drljaca, C. D. Hubbard, R. van Eldik, T. Asano, M. V. Basilevsky, and W. J. le Noble, *Chem. Rev.*, **98**, 2167 (1998).

13 T. Asano, H. Furuta, and H. Sumi, *J. Am. Chem. Soc.*, **116**, 5545 (1994).

14 T. Asano, K. Cosstick, H. Furuta, K. Matsuo, and H. Sumi, *Bull. Chem. Soc. Jpn.*, **69**, 551 (1996).

15 T. Asano, K. Matsuo, and H. Sumi, *Bull. Chem. Soc. Jpn.*, **70**, 239 (1997).

16 Y. Ohga, T. Asano, N. Karger, T. Gross, and H.-D. Lüdemann, *Z. Naturforsch.*, **54a**, 417 (1999).

17 For benzaldehyde anils, see T. Asano, H. Furuta, H.-J. Hofmann, R. Cimiraaglia, Y. Tsuno, and M. Fujio, *J. Org. Chem.*, **58**, 4418 (1993) and earlier papers cited therein.

18 For azobenzenes, see R. Cimiraaglia, T. Asano, and H.-J. Hofmann, *Gazz. Chim. Ital.*, **126**, 679 (1996) and earlier papers cited therein.

19 T. W. Swaddle, H. Doine, S. D. Kinrade, A. Sera, T. Asano, and T. Okada, *J. Am. Chem. Soc.*, **112**, 2378 (1990).

20 K. Stephan and K. Lucas, "Viscosity of Dense Fluids," Plenum, New York (1979).

21 H. A. Kramers, *Physica*, **7**, 284 (1940).

22 R. F. Grote and J. T. Hynes, *J. Chem. Phys.*, **73**, 2715 (1980).

23 As a review, J. T. Hynes, *J. Stat. Phys.*, **42**, 149 (1986).

24 N. Agmon and J. J. Hopfield, *J. Chem. Phys.*, **78**, 6947 (1983).

25 N. Agmon and J. J. Hopfield, *J. Chem. Phys.*, **79**, 2042 (1983).

26 H. Sumi and R. A. Marcus, *J. Chem. Phys.*, **84**, 4894 (1986).

27 H. Sumi, *J. Phys. Chem.*, **95**, 3334 (1991).

28 k_f and k_{TST} in Eq. 5 corresponds to k_1 and $k_1 k_2 / k_{-1}$ in Scheme 1, respectively.

29 M. V. Basilevsky, V. M. Rayboy, and N. N. Weinberg, *J. Phys. Chem.*, **94**, 8734 (1990).

30 M. V. Basilevsky, V. M. Rayboy, and N. N. Weinberg, *J. Phys. Chem.*, **95**, 5533 (1991).

31 There are two papers that reported apparent correlation of the isomerization rate of DODCI with the medium viscosity.^{32,33} Fleming and co-workers³² modified the chain length of 1-alkanol to manipulate the viscosity and Hara and Akimoto³³ applied high pressure. The rate constant decreased with an increase in chain-length/pressure and the results were analyzed on the basis of the KGH model. The highest viscosity reached were in the order of $1 \times 10^{-2} \text{ Pa s}$ in both cases. Although it is not possible to rationalize a small rate decrease with increasing chain length, $k_{\text{EtOH}}/k_{\text{DecOH}} \approx 2$, on the basis of the solvent polarity, in the light of our previous¹³⁻¹⁶ and the present results, it seems to be reasonable to conclude that the solvent/pressure effects they observed were "static" effects as discussed in the introduction.

32 S. P. Velsko, D. H. Waldek, and G. R. Fleming, *J. Chem. Phys.*, **78**, 249 (1983).

33 K. Hara, and S. Akimoto, *J. Phys. Chem.*, **95**, 5811 (1991).

34 T. Asano and T. Okada, *J. Phys. Chem.*, **88**, 238 (1984).

35 J. A. Riddick, W. B. Bunger, and T. K. Sakano, "Techniques of Chemistry Vol. II, Organic Solvents," 4th ed, John Wiley, New York (1986).

36 M. S. Churio, K. P. Angermund, and S. E. Braslavsky, *J. Phys. Chem.*, **98**, 1776 (1994).

37 A major part of the volume increase comes from an increase in the free volume. Therefore, it is usually observed that the compressibility is larger in the activated complex/reactant when the activation volume is positive/negative.

38 C. A. N. Viana and J. C. R. Reis, *Pure Appl. Chem.*, **68**, 1541 (1996).

39 In ethanol, E_a for DODCI was 58.9 kJ mol^{-1} at 0.1 MPa in reasonable agreement with a previously reported value,³² 61.5 kJ mol^{-1} . The value gradually increased with pressure and it was 60.4 kJ mol^{-1} at 600 MPa.